

Published in final edited form as:

*Neuropharmacology*. 2012 February ; 62(2): 890–900. doi:10.1016/j.neuropharm.2011.09.018.

## Recombinant human MFG-E8 attenuates cerebral ischemic injury: its role in anti-inflammation and anti-apoptosis

Cletus Cheyuo, Asha Jacob, Rongqian Wu, Mian Zhou, Lei Qi, Weifeng Dong, Youxin Ji, Wayne W. Chung, Haichao Wang, Jeffrey Nicastro, Gene F. Coppa, and Ping Wang

The Feinstein Institute for Medical Research, Elmezzi Graduate School of Molecular Medicine & Department of Surgery, North Shore University Hospital and Long Island Jewish Medical Center, Manhasset, NY

### Abstract

Excessive inflammation and apoptosis contribute to the pathogenesis of ischemic stroke. MFG-E8 is a 66-kDa glycoprotein that has shown tissue protection in various models of organ injury. However, the potential role of MFG-E8 in cerebral ischemia has not been investigated. We found that levels of MFG-E8 protein in the brain were reduced at 24 h after cerebral ischemia. To assess the potential role of MFG-E8 in cerebral ischemia, adult male Sprague-Dawley rats were subjected to permanent middle cerebral artery occlusion (MCAO). At 1 h post-stroke onset, an intravenous administration of 1 ml saline as vehicle or 160  $\mu\text{g}/\text{kg}$  BW recombinant human MFG-E8 (rhMFG-E8) as treatment was given. The optimal dose of rhMFG-E8 was obtained from previous dose-response organ protection in rat sepsis studies. Neurological scores were determined at 24 h and 48 h post-MCAO. Rats were sacrificed thereafter and brains rapidly removed and analyzed for infarct size, histopathology, and markers of inflammation and apoptosis. Compared with saline vehicle, rhMFG-E8 treatment led to significant decreases in sensorimotor and vestibulomotor deficits, and infarct size at 24 h and 48 h post-MCAO. Measures associated with improved outcome included reduced microglial inflammatory cytokine secretion, adhesion molecules and neutrophil influx, cleaved caspase-3, and upregulation of peroxisome proliferator activated receptor- $\gamma$  (PPAR- $\gamma$ ), and Bcl-2/Bax ratio leading to decreased apoptosis. Thus, rhMFG-E8 treatment is neuroprotective against cerebral ischemia through suppression of inflammation and apoptosis.

### Keywords

MFG-E8; cerebral ischemia; inflammation; apoptosis; neuroprotection

---

© 2011 Elsevier Ltd. All rights reserved.

Please address future correspondences to: Dr. Ping Wang, Center for Immunology and Inflammation, The Feinstein Institute for Medical Research, 350 Community Drive, Manhasset, NY 11030, Tel: (516) 562-3411, Fax: (516) 562-2396, pwang@nshs.edu.

#### DISCLOSURE/CONFLICT OF INTEREST

One of the authors (P Wang) is an inventor of the pending PCT application #WO/2009/064448: "Prevention and treatment of inflammation and organ injury after ischemia/reperfusion using MFG-E8". These patent applications cover the fundamental concept of using MFG-E8 for the treatment of sepsis and ischemia/reperfusion injury. Other authors report no financial conflicts of interest.

**Publisher's Disclaimer:** This is a PDF file of an unedited manuscript that has been accepted for publication. As a service to our customers we are providing this early version of the manuscript. The manuscript will undergo copyediting, typesetting, and review of the resulting proof before it is published in its final citable form. Please note that during the production process errors may be discovered which could affect the content, and all legal disclaimers that apply to the journal pertain.

## INTRODUCTION

Inflammation and apoptosis play crucial roles in the evolution of cerebral infarct following ischemic insult. Following necrotic cell death in the core of the cerebral infarct, cell death in the relatively hypoperfused penumbra occurs over time through inflammatory and apoptotic mechanisms. The inflammatory process involves NF- $\kappa$ B mediated release of cytokines, such as TNF- $\alpha$ , which cause cell injury (Dirnagl *et al.* 1999). Apoptosis involves release of pro-apoptotic molecules such as bax, and activation of the caspases leading to DNA fragmentation and cell death. The cell-damaging mechanisms which are activated by ischemia are countered by cell-survival mechanisms including upregulation of anti-apoptotic molecules such as bcl-2 (Antonsson 2004). The peroxisome-proliferator activated receptor- $\gamma$  (PPAR- $\gamma$ ) is a ligand-inducible transcription factor that has been shown to counteract inflammation by downregulating cytokine release (Ricote and Glass 2007). Therapeutic suppression of inflammation and apoptosis could rescue the penumbra after ischemic stroke.

Milk fat globule-EGF factor VIII (MFG-E8), also known as lactadherin, is a 66-kDa glycoprotein originally discovered in mouse milk and mammary epithelium (Stubbs *et al.* 1990). MFG-E8 was subsequently found to be widely distributed in various tissues in mice and other mammalian species including humans (Aziz *et al.* 2009; Hanayama *et al.* 2004; Larocca *et al.* 1991). In the brain, MFG-E8 is expressed in astrocytes (Boddaert *et al.* 2007) and microglia (Fuller and Van Eldik 2008). MFG-E8 contains two N-terminal epidermal growth factor (EGF)-like repeats, and two C-terminal discoidin/F5/8C domains. MFG-E8 binds  $\alpha_v\beta_{3/5}$  integrin heterodimers through an arginine-glycine-aspartic acid (RGD) motif contained in the second EGF domain (Andersen *et al.* 1997). The second F5/8C domain of MFG-E8 also has high affinity for anionic membrane phospholipids such as phosphatidylserine which become externalized during apoptosis (Andersen *et al.* 1997; Shao *et al.* 2008). MFG-E8 has been shown to facilitate phagocytic removal of apoptotic cells by acting as a bridging molecule between phosphatidylserine exposed on the apoptotic cell and  $\alpha_v\beta_{3/5}$  integrin receptors on phagocytes. This enhanced clearance of apoptotic cells prevents secondary necrosis which could release pro-inflammatory mediators leading to tissue damage (Hanayama *et al.* 2002). MFG-E8 also exerts other beneficial effects in tissue injury such as suppression of inflammation and apoptosis in intestinal ischemia (Cui *et al.* 2010) and Alzheimer's disease (Fuller and Van Eldik 2008). However, the effects of MFG-E8 in cerebral ischemia have not been investigated. Here we show for the first time that brain MFG-E8 levels are reduced after cerebral ischemia, and that administration of recombinant human MFG-E8 (rhMFG-E8) attenuated brain injury by suppressing inflammation and apoptosis.

## MATERIALS AND METHODS

### Experimental animals

Male Sprague-Dawley rats (300 – 350g), purchased from Charles River Laboratories (Wilmington, MA) were used in this study. The rats were housed under standard conditions (room temperature, 22°C, 12/12-h light/dark cycle) with regular access to standard Purina rat chow and water. The animals were allowed at least 5 days to acclimate under these conditions before being used for experiments. All animal experiments were performed in accordance with the National Institutes of Health guidelines for the use of experimental animals. This protocol was approved by the Institutional Animal Care and Use Committee (IACUC) of the Feinstein Institute for Medical Research.

## Model of cerebral ischemia

Rats were fasted overnight but had access to water *ad libitum* before induction of cerebral ischemia. Permanent focal cerebral ischemia was induced by middle cerebral artery occlusion (MCAO) as previously described (Cheyuo *et al.* 2011; Zeng *et al.* 2010) with few modifications. Briefly, anesthesia was induced with 3.5% isoflurane and subsequently maintained by intravenous boluses of pentobarbital, not exceeding 30 mg/kg BW. Body temperature was maintained between 36.5°C and 37.5°C using a rectal temperature probe and a heating pad (Harvard Apparatus, Holliston, MA). The right common carotid artery (CCA) was exposed through a ventral midline neck incision and was carefully dissected free from the vagus nerve. The external carotid artery was then dissected and ligated. The internal carotid artery (ICA) was isolated and carefully separated from the adjacent vagus nerve, and the pterygopalatine artery was dissected and temporally occluded with a microvascular clip. Next, the CCA was ligated and an arteriotomy made just proximal to the bifurcation. A 2.5 cm length of 3-0 poly-L-lysine coated monofilament nylon suture with a rounded tip was inserted through the arteriotomy into the ICA and advanced to the middle cerebral artery (MCA) origin to cause occlusion. Occlusion of the MCA was ascertained by inserting the suture to a predetermined length of 19–20 mm from the carotid bifurcation and feeling for resistance as the rounded suture tip approaches the proximal anterior cerebral artery which is of a relatively narrower caliber. The cervical wound was then closed in layers. One hour post-MCAO each rat was given an infusion of 1 ml saline as vehicle or 160 µg/kg BW rhMFG-E8 as treatment. Rats were then allowed to recover from anesthesia in a warm and quiet environment. The intraluminal suture was left in-situ and rats allowed unrestricted access to food and water. Rats were sacrificed at 24 h or 48 h time points after MCAO. The Bederson neurological deficit scoring scale (no deficit = 0, forelimb flexion = 1, decreased resistance to push = 2, circling = 3) was used to screen rats at 24 h post-operatively for successful MCAO. Rats with a Bederson score of at least 3 were considered to have had successful MCAO as previously described (Kozak *et al.* 2008). Rats with lesser Bederson scores were replaced. Brain tissues were rapidly collected after rats were sacrificed for various analyses. For histopathology, immunohistochemistry and terminal deoxynucleotidyl transferase dUTP nick end labeling (TUNEL), rat brains were transcardially perfused with ice-cold normal saline followed by 4% paraformaldehyde before removal. Brain samples were then paraffin-embedded and sectioned.

## Assessment of brain MFG-E8 levels after cerebral ischemia

To establish a physiological basis for the use of MFG-E8 in the treatment of cerebral ischemia, we assessed changes in brain MFG-E8 protein levels and gene expression after 24 h - cerebral ischemia. MFG-E8 protein levels were determined by Western blot. Briefly, protein obtained from brain homogenates of vehicle and sham groups were fractionated on a Bis-Tris gel and transferred to a 0.22 µm nitrocellulose membrane. Blots were blocked with 10% milk in Tris-buffered saline containing 0.1% vol/vol Tween 20 (TBST) and incubated with goat anti-MFG-E8 polyclonal IgG (1:100 in 10% BSA in TBST). After the incubation with horseradish peroxidase-labeled donkey anti-goat IgG (Santa Cruz Biotechnology Inc., Santa Cruz, CA) in 5% milk in TBST, and subsequently washing with TBST, bands were detected by chemiluminescence (GE Healthcare Biosciences, Piscataway, NJ). The band densities were normalized by β-actin using the Bio-Rad imaging system. MFG-E8 gene expression was measured by real-time PCR. Briefly, total RNA extracted from cerebral cortex and reverse transcribed into cDNA as previously described by us (Wu *et al.* 2009b). MFG-E8 gene expression was then determined from cDNA using murine leukemia virus reverse transcriptase in an Applied Biosystems 7300 real-time PCR system (Applied Biosystems, Foster City, CA). Expression amount of rat glyceraldehyde-3-phosphate dehydrogenase (GAPDH) mRNA was used for normalization of each sample. Relative expression of mRNA was calculated by the  $2^{-\Delta\Delta C_t}$  method, and results expressed as fold

change with respect to control. The following rat primers were used: MFG-E8 (Gene Bank NM\_012811); Forward 5' TGA GGA ACA AGG AAC CAG 3', Reverse: 5' GGA AGG ACA CGC ACA TAG 3'.

### Administration of rhMFG-E8

rhMFG-E8 was used as treatment in this study. rhMFG-E8 was expressed in-house using an *E. coli* system. The Ex-M0438-B01 expression clone for 6xHis-human MFG-E8 was purchased from GeneCopoeia, Inc (Germantown, MD) (Qiang *et al.* 2011Qiang *et al.* in press). rhMFG-E8 was dissolved in sterile normal saline. The dose of rhMFG-E8 used in this study was chosen empirically based on our previous experiments on dose-response effects of rhMFG-E8 in an animal model of sepsis. rhMFG-E8 dose-dependently decreased inflammatory cytokines, markers of organ injury such as transaminases, apoptosis, and mortality in rat sepsis. rhMFG-E8 at a dose of 160 µg/kg BW caused the most reduction in these markers of organ injury and mortality (Shah *et al.* 2011Shah *et al.* in press). rhMFG-E8 was administered through a right femoral vein catheter 1 h post-MCAO. For animals undergoing 48 h – MCAO, a second dose of rhMFG-E8 was given at 24 h post-MCAO, via a left femoral vein catheter. The genomic sequences and amino acid structures of human and mouse MFG-E8 have been well characterized. There is an approximately 68% overall sequence homology between the mouse form of MFG-E8 and the human form (Collins *et al.* 1997). The integrin-binding RGD domain is highly conserved between the mouse and human except for the substitution of valine (V) for isoleucine (I) in the human form, as shown below (in bold font):

CSKNPCHNGGLCEEISQEV**RGD**VFPSYTCTCLKGYAGNHCTKC (human) (Couto *et al.* 1996).

CSPNPCYNDKCLVTLDT**QRGD**IFTEYICQCPVGYSGIH CETGC (mouse) (Stubbs *et al.* 1990).

As a result of the highly conserved structure of the RGD domain, integrin-mediated effects of murine and human MFG-E8 are expected to be similar.

### Blood pressure monitoring

During MCAO surgery, the right femoral artery was catheterized using PE-50 tubing and connected to Digi-Med blood pressure analyzer, BPA-400 (Micro-Med, Inc. Louisville, KY). The mean arterial blood pressure (MABP/mmHg) was monitored continuously during MCAO, and during a 30 minute infusion of rhMFG-E8 or saline vehicle, beginning at 1 h post-MCAO.

### Assessment of neurological deficit

Prior to the induction of stroke by MCAO, rats were trained for two consecutive days on the *modified beam balance test* and the *limb placing test* as previously described (Kawamata *et al.* 1996). Briefly, the modified beam balance test measures vestibulomotor reflex activity when the animal is placed on a narrow beam (30 x 1.3 cm) for 60 seconds. Ability to balance on the beam is scored as follows: animal balances with all four paws on the top of beam = 1; animal puts paws on side of beam or wavers on beam = 2; one or two limbs slip off beam = 3; three limbs slip off beam = 4; animal attempts to balance with paws on beam but falls off = 5; animal drapes over beam, then falls off = 6; animal falls off beam without an attempt to balance = 7. In our training schedule each rat had a total of 20 attempts at balancing on the beam, each lasting 60 seconds; 10 attempts each day. At the end of the 20 attempts each rat attained an average baseline score of 1 before cerebral ischemia is induced.

The limb placing test assesses sensorimotor function. In our experiments we assessed the limb placing test on the left forelimb and hindlimb since we induced right-sided ischemic stroke. Briefly, the forelimb placing test consists of three components – *Visual*, *Tactile*, and *Proprioceptive*. For the visual placing subtest, the rat is held upright by the examiner and brought close to the edge of a table. Immediate placing of the limb on the table is considered normal and scored as 0; delayed placing (<2 seconds) is scored as 1; and no or very delayed placing (>2 s) is scored as 2. Separate scores are obtained for forelimb placing as the rat is brought forward (*Visual-Forward*) and then as the rat is brought sideways (*Visual-Sideways*) to the table (maximum score per forelimb = 4). The tactile placing test is performed by cupping the face of the rat with the hand, covering the eyes and whiskers such that the rat cannot see and the whiskers cannot touch the table. Separate scores are obtained for forelimb placing as the rat is brought forward (*Tactile-Forward*) and then also sideways (*Tactile-Sideways*), in each case with the dorsal forepaw lightly touching the edge of the table (maximum score per forelimb = 4). The proprioceptive placing only involves bringing the rat forward (maximum score per forelimb = 2). The total forelimb placing score is a summation of the visual, tactile and proprioceptive scores (score range 0–10). The hindlimb placing test is conducted in the same manner as above for the forelimbs, but involves only tactile and proprioceptive subtests (maximum scores 4 and 2, respectively; total score range, 0–6). In our experiments each rat received 6 training test; 3 each day. Each rat attained a limb placing score of zero prior to stroke induction. Neurological deficits were determined at 24 h and 48 h post-MCAO.

### Assessment of infarct volume

Infarct size was determined as previously described (Lu *et al.* 2010). Rats were euthanized under anesthesia at 24 h or 48 h post-MCAO. The brains were rapidly removed and sectioned coronally into 2 mm-thick slices which were incubated in 2% triphenyl tetrazolium chloride at 37°C for 30 min and then immersed in 10% formalin overnight. The pale-appearing infarcted areas, as well as areas of the hemispheres were digitally analyzed using NIH Image J software. The infarct volume and volumes of the hemispheres in each slice were calculated as the area multiplied by 2. The total infarct volume and hemispheric volumes for each rat brain were calculated as summation of the individual slices. An edema index was calculated by dividing the total volume of the right hemisphere (ischemic side) by the total volume of the left hemisphere (non-ischemic side). The actual infarct volume adjusted for edema was calculated by dividing the infarct volume by the edema index, and expressed as percentage of the total brain volume.

### Histopathological assessment

6 µm thick paraffin-embedded sections were stained with hematoxylin and eosin (H&E). The H&E stained slides were examined under bright field microscopy. The ischemic core and the penumbra were first identified using the 4× objective (Nikon Eclipse Ti microscope, Japan). An area was then identified in the penumbra and examined at a higher magnification, using the 40× objective, for basophilic neurons, with purple-blue cytoplasm, and eosinophilic neurons, with pink cytoplasm, which are classified as intact neurons and necrotic neurons respectively (Ozden *et al.* 2011). Four sections, one per animal, taken at the same coronal level, were analyzed for each group. Six images from six random visual fields were taken per slide. Quantification of intact neurons was performed by co-author L.Q., who was blinded to treatment allocations and functional outcomes. The average intact neuron count for each slide was expressed as intact neurons per 40× high power field.

### BV2 microglia oxygen – glucose deprivation (OGD)

BV2 microglial cells were cultured in Dulbecco's Modified Eagle Medium (DMEM) supplemented with 10% fetal bovine serum (FBS), 1% penicillin-streptomycin, and 1%

glutamine, as previously described (Boscia *et al.* 2009). Briefly, cells were plated in triplicates at  $2 \times 10^6$  per well (six well plates) in DMEM containing glucose and supplemented with FBS, penicillin-streptomycin, and glutamine. Plated cells were then incubated at 37 °C, 5% CO<sub>2</sub> overnight to enable attachment. The next day the culture medium was changed to glucose-free DMEM supplemented with FBS and penicillin-streptomycin. The treatment group had 0.5 µg/ml rhMFG-E8 added to the medium, while phosphate buffered saline (PBS) was added to the vehicle group. The culture plates were then placed in an air-tight hypoxia chamber (Billups-Rothenberg, Inc., Del Mar, CA) in which the atmosphere was saturated with 95%N/5%CO<sub>2</sub> and then incubated at 37 °C for 24 h. To mimic the permanent MCAO model, supernatants were collected for analysis after 24 h oxygen-glucose deprivation, without re-oxygenation. Control cells were plated in glucose-containing DMEM and incubated under normoxia at 37°C, 5% CO<sub>2</sub> for 24 h. Three separate BV2 microglia-OGD experiments, in triplicates, were performed.

#### Determination of cerebral interleukin-6 levels

Interleukin-6 (IL-6) levels in brain tissue lysates from the ipsilateral cerebral cortex and BV2 microglia-OGD supernatants were quantified by using commercially obtained enzyme-linked immunosorbent assay (ELISA) kits specific for IL-6 (BD BioSciences, San Jose, CA). The assay was carried out according to the instructions provided by the manufacturer.

#### Determination of cerebral TNF-α and myeloperoxidase (MPO) levels by immunohistochemistry

6 µm paraffin sections of brain tissue were de-waxed and rehydrated, followed by microwave antigen retrieval procedure. Endogenous peroxidase and nonspecific binding sites were blocked using 2% H<sub>2</sub>O<sub>2</sub> in 60% methanol and 3% normal goat serum respectively. The sections were then incubated with the following primary antibodies at room temperature for 2 h: rabbit anti-TNF-α polyclonal IgG (1:100, Millipore, Temecula, CA), and rabbit anti-MPO polyclonal IgG (1:100, Abcam, Cambridge, MA). The sections were then reacted with biotinylated anti-rabbit IgG, Vectastain ABC and DAB reagents (Vector Labs, Burlingame, CA). The immunohistochemical reaction was examined under light microscopy at 400× original magnification (Nikon E600 microscope, Japan). Neutrophils appeared as small, round, MPO-staining cells. Six sections, one per animal, taken from the same coronal level, were analyzed for each group. Six images from six random fields in the penumbra of each slide were obtained. The average number of neutrophils was determined by NIH ImageJ particle analysis and expressed as neutrophils per 40× high power field.

#### Determination of ICAM-1 gene expression

Total RNA extracted from cerebral cortex by Tri-Reagent (Molecular Research Center, Cincinnati, OH) was reverse transcribed into cDNA and real-time PCR performed as previously described by us (Wu *et al.* 2009b). Briefly, ICAM-1 gene expression was determined from cDNA using murine leukemia virus reverse transcriptase in an Applied Biosystems 7300 real-time PCR system (Applied Biosystems, Foster City, CA). Expression amount of rat glyceraldehyde-3-phosphate dehydrogenase (GAPDH) mRNA was used for normalization of each sample. Relative expression of mRNA was calculated by the  $2^{-\Delta\Delta Ct}$  method, and results expressed as fold change with respect to control. The following rat primers were used: *ICAM-1*(NM\_012967.1); Forward: 5' CGA GTG GAC ACA ACT GGA AG 3', Reverse: 5' CGC TCT GGG AAC GAA TAC AC 3'.

### Western blot for peroxisome proliferator-activated receptor- $\gamma$ (PPAR- $\gamma$ ), cleaved caspase-3, Bcl-2 and Bax

Protein from homogenates of the ipsilateral cerebral cortex were fractionated on Bis-Tris gel and transferred to nitrocellulose (PPAR- $\gamma$ ) or PVDF (cleaved caspase-3, bcl-2, and bax) membrane. The membranes were blocked in 5% milk in TBST (Tris-buffered saline Tween 20) and incubated overnight at 4°C with the following rabbit polyclonal antibodies: anti-PPAR- $\gamma$  (1: 1000, Cayman Chemical, Ann Arbor, MI), anti-cleaved caspase-3 (1: 500, Cell Signaling Technology, Danvers, MA), anti-Bcl-2, and anti-Bax (1: 500, Santa Cruz Biotechnology, Santa Cruz, CA). After reacting blots with HRP-labeled goat anti-rabbit IgG, protein bands were detected by chemiluminescence (GE Healthcare Biosciences, Piscataway, NJ). The band densities were normalized by  $\beta$ -actin using the Bio-Rad imaging system.

### TUNEL assay

6  $\mu$ m paraffin sections of brain tissue were dewaxed and rehydrated. Tissue sections were then incubated with proteinase K, 15.3 mg/mL in Tris buffer, pH 8, for 20 min at room temperature and rinsed with 50 mM TBS, pH 7.6. The sections were then reacted with a green fluorescent-tagged enzyme solution (Roche Diagnostics, Indianapolis, IN). The slides were then washed with TBS, mounted with Vectashield medium with propidium iodide (Vector labs, Burlingame, CA) and examined under a fluorescence microscope (Nikon E600 microscope, Japan). Apoptotic cells appeared green fluorescent, and the nuclei which appeared red fluorescent confirmed the nuclear location of TUNEL products. Six sections, one per animal, taken from the same coronal level, were analyzed for each group. Eight images were obtained from eight random visual fields in the penumbra of each slide at 200 $\times$  original magnification. The average number of TUNEL positive cells for each slide was quantified by NIH ImageJ particle analysis and expressed as TUNEL positive cells per 20 $\times$  high power field.

### 48-hour survival study

A survival analysis was performed for the 48 h –MCAO time point experiments. Animals were observed every 12 hours for mortality. Dead animals in each group were replaced until there were 5 surviving animals per group at 48 hours post-MCAO. Immediately prior to sacrifice, neurological deficit assessment by beam balance test was performed on the surviving animals as described above. Two separate experiments were conducted; the first set of experiments was conducted to obtain brain sample for infarct size analysis at 48 h – post MCAO, and the second set of experiments to obtain brain sample for protein analysis.

### Statistical analysis

All data are expressed as means  $\pm$  SE and compared Student's *t*-test for two groups, and analysis of variance (ANOVA) and the Student-Newman-Keuls method for multiple groups or Kruskal-Wallis one-way ANOVA on ranks. Short term survival rate was estimate by Kaplan-Meier LogRank analysis. Differences in values were considered significant at  $p < 0.05$ .

## RESULTS

### Cerebral MFG-E8 protein levels are reduced by cerebral ischemia

To determine whether permanent cerebral ischemia altered brain MFG-E8 levels, we measured cerebral MFG-E8 protein levels and gene expression at 24 h post-MCAO. As shown in Figure 1a, MCAO decreased cerebral MFG-E8 protein levels by 32.7% compared with sham ( $p < 0.05$ ). The gene expression of MFG-E8 was, however, not altered by cerebral

ischemia (Figure 1b), suggesting a post-translational mechanism for the decrease in MFG-E8 protein level during cerebral ischemia. MFG-E8 has been shown to undergo proteasomal degradation (Zimmerman *et al.* 2011), and proteasome is activated during cerebral ischemia (Kleinschnitz *et al.* 2011). Thus, we speculate that the decreased MFG-E8 protein level in cerebral ischemia is probably as a result of proteasomal degradation.

### **rhMFG-E8 does not alter blood pressure in ischemic stroke**

To assure that rhMFG-E8 does not cause adverse hemodynamic changes when used for the treatment of cerebral ischemia, blood pressure was monitored during a 30 minute intravenous infusion at 1 h post-MCAO. As shown in Figure 2, rhMFG-E8 infusion did not alter the mean arterial blood pressure compared with saline vehicle.

### **rhMFG-E8 treatment improves neurological function**

Animals developed sensorimotor and vestibulomotor deficits at both 24 h and 48 h time points after MCAO. As shown in Figure 3a, rhMFG-E8 treatment reduced left forelimb sensorimotor deficit, measured by the limb placing test, by 30.7% at 24 h post-MCAO compared with the vehicle group ( $p < 0.05$ ). rhMFG-E8 treatment also decreased left hindlimb sensorimotor deficit by 27.3% at 24 h post-MCAO, though not significant compared to vehicle (Figure 3b). Vestibulomotor deficit, measured by beam balance test, was significantly reduced by rhMFG-E8 treatment by 25.6% and 36% at 24 h and 48 h post-MCAO respectively, compared with vehicle (Figures 3c and d,  $p < 0.05$ ). In the vehicle group, vestibulomotor deficit worsened from 24 h time point to the 48 h time point after MCAO ( $4.3 \pm 0.3$  vs.  $5 \pm 0.3$ ), though not statistically significant. rhMFG-E8 treatment maintained vestibulomotor deficit at  $3.2 \pm 0.2$  from 24 h to 48 h time point after MCAO.

### **rhMFG-E8 decreases infarct size**

Infarct size was measured at 24 h and 48 h time points after cerebral ischemia. In the vehicle group, 24 hours of cerebral ischemia by MCAO caused infarction of 29.3% of the ipsilateral cerebral hemisphere. rhMFG-E8 treatment decreased the infarct size by 28.3% compared with vehicle ( $p < 0.05$ , Figure 4a). At 48 h post-MCAO, rhMFG-E8 also decreased the infarct size by 33.1% compared with vehicle ( $p < 0.05$ , Figure 4b). Representative images of TTC stain for infarct size are shown in Figure 4c. The infarct size did not change significantly from 24 h post MCAO to 48 h post-MCAO in both vehicle group ( $29.3 \pm 1.3$  vs.  $29 \pm 1.5$ ) and rhMFG-E8 group ( $21 \pm 1.3$  vs.  $19.4 \pm 3.6$ ). This is consistent with previous histological (Kaplan *et al.* 1991; Memezawa *et al.* 1992) and imaging (Hofmeijer *et al.* 2004) time-course assessments of infarct size, which showed that the infarct size does not increase beyond 24 h after a permanent cerebral ischemic insult.

### **rhMFG-E8 decreases neuronal necrosis in the penumbra**

Twenty four hours of cerebral ischemia by MCAO resulted in profound neuronal necrosis in the ischemic core and the penumbra, appearing as eosinophilic neurons on hematoxylin-eosin staining (Figure 5a). Treatment with rhMFG-E8 protected neurons from necrosis, preserving 25% (expressed as a percent of sham) of intact basophilic neurons in the penumbra compared to 7% in vehicle ( $p < 0.05$ , Figure 5b).

### **rhMFG-E8 suppresses inflammation in cerebral ischemia**

IL-6 secretion has been shown to peak at 24 h after permanent focal cerebral ischemia (Legos *et al.* 2000). We found that 24 h - MCAO resulted in elevations of cerebral IL-6 levels by 321% and 154% in vehicle and rhMFG-E8 treated animals respectively compared with sham animals. Treatment with rhMFG-E8 decreased IL-6 levels by 39.6% compared with vehicle ( $p < 0.05$ , Figure 6a). Since microglia, the residential macrophages in the brain,



are the presumable source of IL-6, we measured IL-6 secretion in BV2 microglia – OGD, without re-oxygenation, to mimic the permanent MCAO model. In three separate experiments, rhMG-E8 significantly decreased IL-6 levels in the supernatants. Figure 6b, which represents the means of the averages of the three experiments, shows that rhMFG-E8 decreased the IL-6 level by 31.6% compared with phosphate buffered saline (PBS) treatment. Cerebral TNF- $\alpha$  level immunohistochemistry also showed decreased expression (less intensity of staining) in rhMFG-E8 treatment compared with vehicle animals (Figure 6c). An assessment of cerebral neutrophil infiltration as part of the inflammatory response showed that rhMFG-E8 treatment also decreased the number of infiltrated neutrophils compared with vehicle at 24 h post-MCAO (Figure 6d). In fact, Figure 6e shows that rhMFG-E8 decreased the neutrophil infiltration by 37.2% compared with vehicle ( $p < 0.05$ ). Expression of ICAM-1, an adhesion molecule involved in neutrophil infiltration (Wiessner *et al.* 2009), was upregulated in vehicle group compared with sham ( $p < 0.05$  vs. Sham, Figure 6f). We found that rhMFG-E8 treatment decreased ICAM-1 gene expression by 31.6%, even though this downregulation was not significant compared with vehicle. We also found that MCAO downregulated the ligand-inducible transcription factor, PPAR- $\gamma$ , in vehicle and rhMFG-E8 treated animals compared with sham. rhMFG-E8 treatment increased PPAR- $\gamma$  levels by 39.3% compared with the vehicle group ( $p < 0.05$ , Figure 6g). PPAR- $\gamma$  inhibits the expression of early inflammatory response genes including cytokines such as IL-6 (Yu *et al.* 2008). Thus, the mechanism of rhMFG-E8 anti-inflammatory effects may in part be due to upregulation of PPAR- $\gamma$ .

### rhMFG-E8 inhibits apoptosis in cerebral ischemia

Apoptosis was assessed by measurements of cleaved caspase-3, bcl-2, bax, and TUNEL staining. rhMFG-E8 decreased cleaved caspase-3 levels by 58.7% compared with vehicle at 24 h post-MCAO ( $p < 0.05$ , Figure 7a). At 48 h post-MCAO, rhMFG-E8-mediated suppression of cleaved caspase-3 was not statistically significant compared with vehicle (Figure 7b). Figure 7c shows that 24 h – MCAO decreased the anti-apoptotic bcl-2 levels by 13.1% in the vehicle group compared with sham. rhMFG-E8 treatment on the other hand increased bcl-2 levels by 20.5% compared with vehicle. These changes in bcl-2 levels were however not significant. Figure 7d shows the levels of bax, which is pro-apoptotic, at 24 h post-MCAO. The levels of bax in the sham and vehicle groups are statistically similar. In contrast, rhMFG-E8 significantly suppressed bax levels compared with both vehicle and sham ( $p < 0.05$ , Figure 7d). The combined effect of rhMFG-E8-mediated increase in bcl-2 and decrease in bax leads to a significantly increased bcl-2/bax ratio compared with vehicle and sham ( $p < 0.05$ , Figure 7e). The bcl-2/bax ratio of the sham is about the same as the vehicle. We speculate that the 24 h time point may be relatively too early with regards to bcl-2/bax regulation in cerebral ischemia, such that the changes in vehicle are minimal and similar to baseline levels in sham. rhMFG-E8, a ligand of  $\alpha_v\beta_3$  integrin receptor, on the other hand is expected to have an early effect on bcl-2/bax regulation since  $\alpha_v\beta_3$  integrin receptor signaling has been shown to increase Bcl-2 transcription through a focal adhesion kinase (FAK)-dependent activation of the PI3K-Akt pathway (Matter and Ruoslahti 2001). Consistent with our speculation, at a later time point, 48 h post-MCAO, bcl-2 levels were significantly downregulated in the vehicle compared with sham ( $p < 0.05$ , Figure 7f). At this later time point rhMFG-E8 treatment also significantly upregulated bcl-2 compared with vehicle ( $p < 0.05$ , Figure 7f). Figure 7g shows that bax levels in the vehicle were upregulated by 21.9% compared with sham ( $p < 0.05$ ). rhMFG-E8 treatment downregulated bax levels by 23.4% compared with vehicle ( $p < 0.05$ , Figure 7g). The combined effect of bcl-2 downregulation and bax upregulation in the vehicle group at the later time point of 48 h post-MCAO leads to a significant reduction in bcl-2/bax ratio by 29.7% compared with sham ( $p < 0.05$ , Figure 7h). rhMFG-E8 treatment increased the bcl-2/bax ratio by 51.9% compared with vehicle ( $p < 0.05$ , Figure 7h). Consistent with the anti-apoptotic suppression

of cleaved caspase-3 and upregulation of bcl-2/bax ratio by rhMFG-E8, we found that TUNEL staining of brain sections showed fewer positive cells in the rhMFG-E8 treatment group compared with vehicle ( $p < 0.05$ , Figures 8a and b).

### Short term survival

As shown in Figure 9, mortality during the 48 h – MCAO started earlier in the vehicle group. The overall survival rate in the vehicle group was 50% compared with 77% for rhMFG-E8 treatment ( $p = 0.078$ ).

## DISCUSSION

The MFG-E8 gene, which in humans is located at the chromosomal position 15q25 (Collins *et al.* 1997), is ubiquitously expressed in various tissues, including the brain, in mammals (Aziz *et al.* 2009; Hanayama *et al.* 2004; Larocca *et al.* 1991). MFG-E8 plays physiological roles in cell-cell interaction through the binding of  $\alpha_v\beta_{3/5}$  integrin receptors (Raymond *et al.* 2010). Under pathological conditions, MFG-E8 has been shown to promote clearance of apoptotic cells by binding phosphatidylserine exposed on the apoptotic cells and simultaneously engaging the  $\alpha_v\beta_{3/5}$  integrin receptor on macrophages (Hanayama *et al.* 2002). Apoptotic cells undergo secondary necrosis leading to the release of damage associated molecular pattern (DAMP) molecules which promote inflammation and tissue injury (Miksa *et al.* 2006). Promotion of apoptotic clearance has been shown to be beneficial in various brain diseases. MFG-E8 levels are reduced in Alzheimer's disease, and decreased MFG-E8 mediated clearance of apoptotic neurons and amyloid  $\beta$ -peptides have been shown to play pathogenetic roles in Alzheimer's disease (Boddaert *et al.* 2007). The macrophage scavenger receptor A (CD204), which acts similar to MFG-E8 by promoting macrophage clearance of apoptotic cells, has been shown to be neuroprotective in focal cerebral ischemia (Lu *et al.* 2010). However, the effects of MFG-E8 on cerebral ischemia have not been previously investigated. This study has established for the first time a beneficial role of rhMFG-E8 in focal cerebral ischemia through suppression of inflammation and apoptosis.

We found that at 24 h after the onset of cerebral ischemia, brain MFG-E8 protein levels were significantly reduced compared to baseline sham levels. We found that the gene expression of MFG-E8 was not affected by permanent cerebral ischemia. We suggest that MFG-E8 protein levels may be post-translationally reduced by proteasomal degradation since MFG-E8 has been shown to undergo proteasomal degradation (Zimmerman *et al.* 2011), and proteasome is activated during cerebral ischemia (Kleinschnitz *et al.* 2011). Intravenously administered rhMFG-E8 will not be degraded by proteasome since proteasomal activity occurs intracellularly. In our study, intravenous administration of exogenous rhMFG-E8 one hour after the ischemia reduced infarct size and improved neurological function at both 24 h and 48 h time points after the onset of cerebral ischemia. Histopathological examination also showed that rhMFG-E8 treatment protected neurons in the penumbra against necrosis at 24 h after cerebral ischemia onset. Inflammation (Schilling *et al.* 2003) and apoptosis (Broughton *et al.* 2009) play crucial roles in tissue damage during cerebral ischemia. In the permanent animal model of cerebral ischemia, IL-6 secretion has been shown to peak at 24 hours after cerebral ischemia onset (Legos *et al.* 2000). We demonstrated that the anti-inflammatory effects of rhMFG-E8 treatment in cerebral ischemia included suppression of cytokine (IL-6 and TNF- $\alpha$ ) release, ICAM-1 expression, and cerebral neutrophil infiltration at 24 h after permanent cerebral ischemia. The anti-inflammatory suppression of cytokine release is likely due to the effect of rhMFG-E8 on microglia cells, the resident macrophages in the brain. We confirmed this hypothesis by demonstrating that rhMFG-E8 suppressed IL-6 production during BV2 microglia oxygen-glucose deprivation. The exact signaling mechanism of rhMFG-E8-mediated cytokine downregulation is unknown. Upregulation of the ligand-inducible transcription factor,

PPAR- $\gamma$ , may be responsible for the inhibition of cytokine release following treatment with rhMFG-E8. We found that focal cerebral ischemia by MCAO suppressed PPAR- $\gamma$  levels. Treatment with rhMFG-E8 attenuated the ischemia-induced downregulation of PPAR- $\gamma$  compared with vehicle. PPAR- $\gamma$  is known to suppress NF- $\kappa$ B mediated cytokine production through a variety of mechanisms collectively termed transrepression (Ricote and Glass 2007). PPAR- $\gamma$  agonists such as the thiazolidinediones have shown neuroprotection in cerebral ischemia (Wang *et al.* 2009). Our finding of rhMFG-E8 mediated upregulation of PPAR- $\gamma$  together with suppression of cytokine release is consistent with the work of Zhang *et al* who showed that the PPAR- $\gamma$  agonist, pioglitazone, suppresses NF- $\kappa$ B signaling in permanent focal cerebral ischemia, resulting in neuroprotection (Zhang *et al.* 2011).

We also demonstrated that rhMFG-E8 treatment inhibited apoptosis in cerebral ischemia by downregulating cleaved caspase-3 and bax, and upregulating bcl-2 and bcl-2/bax ratio. We found that bcl-2/bax regulation in permanent focal cerebral ischemia was time-dependent, with a significant decrease in bcl-2/bax ratio in the vehicle group at 48 h post-MCAO compared with sham, in contrast with an earlier time point of 24 h post-MCAO when there was no difference between bcl-2/bax ratio in sham and vehicle group. rhMFG-E8 treatment had an early effect on bcl-2/bax regulation resulting in a persistent significantly increased bcl-2/bax ratio at both 24 h and 48 h after the onset of cerebral ischemia. Upregulation of the Bcl-2/Bax ratio by rhMFG-E8 may be integrin-mediated. The MFG-E8 receptor,  $\alpha_v\beta_3$ , has been shown to increase Bcl-2 transcription through a focal adhesion kinase (FAK)-dependent activation of the PI3K-Akt pathway (Matter and Ruoslahti 2001). The anti-apoptotic effect of rhMFG-E8 may further be explained by the upregulation of PPAR- $\gamma$ . Wu *et al* showed that PPAR- $\gamma$  overexpression inhibited apoptosis in cerebral ischemia. Knockdown of PPAR- $\gamma$  using small interfering RNA abrogated the anti-apoptotic effects of PPAR- $\gamma$  (Wu *et al.* 2009a).

The CX3X chemokine, fractalkine, stimulates the release of MFG-E8 from microglial cells (Leonardi-Essmann *et al.* 2005). The neuroprotective effects of MFG-E8 under conditions of hypoxia/ischemia are further supported by in vitro studies by other investigators using fractalkine. Noda *et al* showed that fractalkine decreased excitotoxicity by stimulating microglial clearance of apoptotic neurons. Treatment of the microglial cells with anti-MFG-E8 neutralizing antibodies abolished the microglial clearance of necrotic neurons and diminished the neuroprotection (Noda *et al.* 2011). Similarly, Kranich *et al* also showed that MFG-E8 protects against neurotoxicity in a model of prion disease (Kranich *et al.* 2010).

In summary, we have shown in this first assessment of the role of rhMFG-E8 in cerebral ischemia that endogenous brain MFG-E8 levels are post-translationally decreased by cerebral ischemia. Exogenous rhMFG-E8, administered intravenously 1 h post cerebral ischemia onset, improved neurological function by suppressing inflammation and apoptosis at the 24 h and 48 h time points after permanent focal cerebral ischemia onset, without altering the hemodynamic status of animals. In accordance with the recommendations of the Stroke Academic and Industrial Roundtable (STAIR) recommendations (Fisher *et al.* 2009), the effects of rhMFG-E8 need to be further assessed independently in the transient focal cerebral ischemia model which includes the additional pathophysiology of reperfusion injury. In conclusion, the current study has shown that rhMFG-E8 is a novel neuroprotective agent for cerebral ischemia, which needs further preclinical development.

## References

- Andersen MH, Berglund L, Rasmussen JT, Petersen TE. Bovine PAS-6/7 binds alpha v beta 5 integrins and anionic phospholipids through two domains. *Biochemistry.* 1997; 36:5441–5446. [PubMed: 9154926]

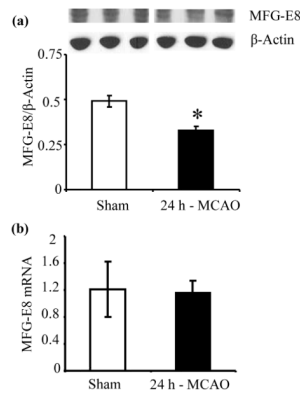
- Antonsson B. Mitochondria and the Bcl-2 family proteins in apoptosis signaling pathways. *Mol Cell Biochem.* 2004; 256–257:141–155.
- Aziz MM, Ishihara S, Mishima Y, Oshima N, Moriyama I, Yuki T, Kadowaki Y, Rumi MA, Amano Y, Kinoshita Y. MFG-E8 attenuates intestinal inflammation in murine experimental colitis by modulating osteopontin-dependent alphavbeta3 integrin signaling. *J Immunol.* 2009; 182:7222–7232. [PubMed: 19454719]
- Boddaert J, Kinugawa K, Lambert JC, Boukhtouche F, Zoll J, Merval R, Blanc-Brude O, Mann D, Berr C, Vilar J, Garabedian B, Journiac N, Charue D, Silvestre JS, Duyckaerts C, Amouyel P, Mariani J, Tedgui A, Mallat Z. Evidence of a role for lactadherin in Alzheimer's disease. *Am J Pathol.* 2007; 170:921–929. [PubMed: 17322377]
- Boscica F, Gala R, Pannaccione A, Secondo A, Scorziello A, Di RG, Annunziato L. NCX1 expression and functional activity increase in microglia invading the infarct core. *Stroke.* 2009; 40:3608–3617. [PubMed: 19745171]
- Broughton BR, Reutens DC, Sobey CG. Apoptotic mechanisms after cerebral ischemia. *Stroke.* 2009; 40:e331–e339. [PubMed: 19182083]
- Cheyuo C, Wu R, Zhou M, Jacob A, Coppa G, Wang P. Ghrelin suppresses inflammation and neuronal nitric oxide synthase in focal cerebral ischemia via the vagus nerve. *Shock.* 2011; 35:258–265. [PubMed: 20720512]
- Collins C, Nehlin JO, Stubbs JD, Kowbel D, Kuo WL, Parry G. Mapping of a newly discovered human gene homologous to the apoptosis associated-murine mammary protein, MFG-E8, to chromosome 15q25. *Genomics.* 1997; 39:117–118. [PubMed: 9027496]
- Couto JR, Taylor MR, Godwin SG, Ceriani RL, Peterson JA. Cloning and sequence analysis of human breast epithelial antigen BA46 reveals an RGD cell adhesion sequence presented on an epidermal growth factor-like domain. *DNA Cell Biol.* 1996; 15:281–286. [PubMed: 8639264]
- Cui T, Miksa M, Wu R, Komura H, Zhou M, Dong W, Wang Z, Higuchi S, Chaung W, Blau SA, Marini CP, Ravikumar TS, Wang P. Milk fat globule epidermal growth factor 8 attenuates acute lung injury in mice after intestinal ischemia and reperfusion. *Am J Respir Crit Care Med.* 2010; 181:238–246. [PubMed: 19892861]
- Dirnagl U, Iadecola C, Moskowitz MA. Pathobiology of ischaemic stroke: an integrated view. *Trends Neurosci.* 1999; 22:391–397. [PubMed: 10441299]
- Fisher M, Feuerstein G, Howells DW, Hurn PD, Kent TA, Savitz SI, Lo EH. Update of the stroke therapy academic industry roundtable preclinical recommendations. *Stroke.* 2009; 40:2244–2250. [PubMed: 19246690]
- Fuller AD, Van Eldik LJ. MFG-E8 regulates microglial phagocytosis of apoptotic neurons. *J Neuroimmune Pharmacol.* 2008; 3:246–256. [PubMed: 18670887]
- Hanayama R, Tanaka M, Miwa K, Shinohara A, Iwamatsu A, Nagata S. Identification of a factor that links apoptotic cells to phagocytes. *Nature.* 2002; 417:182–187. [PubMed: 12000961]
- Hanayama R, Tanaka M, Miyasaka K, Aozasa K, Koike M, Uchiyama Y, Nagata S. Autoimmune disease and impaired uptake of apoptotic cells in MFG-E8-deficient mice. *Science.* 2004; 304:1147–1150. [PubMed: 15155946]
- Hofmeijer J, Veldhuis WB, Schepers J, Nicolay K, Kappelle LJ, Bar PR, van der Worp HB. The time course of ischemic damage and cerebral perfusion in a rat model of space-occupying cerebral infarction. *Brain Res.* 2004; 1013:74–82. [PubMed: 15196969]
- Kaplan B, Brint S, Tanabe J, Jacewicz M, Wang XJ, Pulsinelli W. Temporal thresholds for neocortical infarction in rats subjected to reversible focal cerebral ischemia. *Stroke.* 1991; 22:1032–1039. [PubMed: 1866750]
- Kawamata T, Alexis NE, Dietrich WD, Finklestein SP. Intracisternal basic fibroblast growth factor (bFGF) enhances behavioral recovery following focal cerebral infarction in the rat. *J Cereb Blood Flow Metab.* 1996; 16:542–547. [PubMed: 8964792]
- Kleinschnitz C, Blecharz K, Kahles T, Schwarz T, Kraft P, Gobel K, Meuth SG, Burek M, Thum T, Stoll G, Forster C. Glucocorticoid insensitivity at the hypoxic blood-brain barrier can be reversed by inhibition of the proteasome. *Stroke.* 2011; 42:1081–1089. [PubMed: 21330632]

- Kozak W, Kozak A, Johnson MH, Elewa HF, Fagan SC. Vascular protection with candesartan after experimental acute stroke in hypertensive rats: a dose-response study. *J Pharmacol Exp Ther*. 2008; 326:773–782. [PubMed: 18559971]
- Kranich J, Krautler NJ, Falsig J, Ballmer B, Li S, Hutter G, Schwarz P, Moos R, Julius C, Miele G, Aguzzi A. Engulfment of cerebral apoptotic bodies controls the course of prion disease in a mouse strain-dependent manner. *J Exp Med*. 2010; 207:2271–2281. [PubMed: 20837697]
- Larocca D, Peterson JA, Urrea R, Kuniyoshi J, Bistrain AM, Ceriani RL. A Mr 46,000 human milk fat globule protein that is highly expressed in human breast tumors contains factor VIII-like domains. *Cancer Res*. 1991; 51:4994–4998. [PubMed: 1909932]
- Legos JJ, Whitmore RG, Erhardt JA, Parsons AA, Tuma RF, Barone FC. Quantitative changes in interleukin proteins following focal stroke in the rat. *Neurosci Lett*. 2000; 282:189–92. [PubMed: 10717423]
- Leonardi-Essmann F, Emig M, Kitamura Y, Spanagel R, Gebicke-Haerter PJ. Fractalkine-upregulated milk-fat globule EGF factor-8 protein in cultured rat microglia. *J Neuroimmunol*. 2005; 160:92–101. [PubMed: 15710462]
- Lu C, Hua F, Liu L, Ha T, Kalbfleisch J, Schweitzer J, Kelley J, Kao R, Williams D, Li C. Scavenger receptor class-A has a central role in cerebral ischemia-reperfusion injury. *J Cereb Blood Flow Metab*. 2010; 30:1972–1981. [PubMed: 20424635]
- Matter ML, Ruoslahti E. A signaling pathway from the alpha5beta1 and alpha(v)beta3 integrins that elevates bcl-2 transcription. *J Biol Chem*. 2001; 276:27757–27763. [PubMed: 11333270]
- Memezawa H, Smith ML, Siesjo BK. Penumbra tissues salvaged by reperfusion following middle cerebral artery occlusion in rats. *Stroke*. 1992; 23:552–559. [PubMed: 1561688]
- Miksa M, Wu R, Dong W, Das P, Yang D, Wang P. Dendritic cell-derived exosomes containing milk fat globule epidermal growth factor-factor VIII attenuate proinflammatory responses in sepsis. *Shock*. 2006; 25:586–593. [PubMed: 16721266]
- Noda M, Doi Y, Liang J, Kawanokuchi J, Sonobe Y, Takeuchi H, Mizuno T, Suzumura A. Fractalkine attenuates excitotoxicity via microglial clearance of damaged neurons and antioxidant enzyme heme oxygenase-1 expression. *J Biol Chem*. 2011; 286:2308–2319. [PubMed: 21071446]
- Ozden H, Durmaz R, Kanbak G, Uzuner K, Aral E, Kartkaya K, Kabay SC, Atasoy MA. Erythropoietin prevents nitric oxide and cathepsin-mediated neuronal death in focal brain ischemia. *Brain Res*. 2011; 1370:185–193. [PubMed: 21108937]
- Qiang X, Li J, Wu R, Ji Y, Chaung W, Dong W, Wang P. Expression and characterization of recombinant human milk fat globule-EGF factor VIII. *Int J Mol Med*. 2011 In press.
- Raymond AS, Elder B, Ensslin M, Shur BD. Loss of SED1/MFG-E8 results in altered luminal physiology in the epididymis. *Mol Reprod Dev*. 2010; 77:550–563. [PubMed: 20422713]
- Ricote M, Glass CK. PPARs and molecular mechanisms of transrepression. *Biochim Biophys Acta*. 2007; 1771:926–935. [PubMed: 17433773]
- Schilling M, Besselmann M, Leonhard C, Mueller M, Ringelstein EB, Kiefer R. Microglial activation precedes and predominates over macrophage infiltration in transient focal cerebral ischemia: a study in green fluorescent protein transgenic bone marrow chimeric mice. *Exp Neurol*. 2003; 183:25–33. [PubMed: 12957485]
- Shah KG, Wu R, Jacob A, Molmenti EP, Nicastro J, Coppa GF, Wang P. Recombinant human milk fat globule-EGF factor 8 produces dose-dependent benefits in sepsis. *Intensive Care Med*. 2011 In press.
- Shao C, Novakovic VA, Head JF, Seaton BA, Gilbert GE. Crystal structure of lactadherin C2 domain at 1.7 Å resolution with mutational and computational analyses of its membrane-binding motif. *J Biol Chem*. 2008; 283:7230–7241. [PubMed: 18160406]
- Stubbs JD, Lekutis C, Singer KL, Bui A, Yuzuki D, Srinivasan U, Parry G. cDNA cloning of a mouse mammary epithelial cell surface protein reveals the existence of epidermal growth factor-like domains linked to factor VIII-like sequences. *Proc Natl Acad Sci U S A*. 1990; 87:8417–8421. [PubMed: 2122462]
- Wang CX, Ding X, Noor R, Pegg C, He C, Shuaib A. Rosiglitazone alone or in combination with tissue plasminogen activator improves ischemic brain injury in an embolic model in rats. *J Cereb Blood Flow Metab*. 2009; 29:1683–1694. [PubMed: 19553906]

- Wiessner R, Eisold S, Linnebacher M, Bungler C, Nizze H, Wacke R, Benz S, Schareck W, Klar E. Up-regulation of ICAM-1 during cold ischemia triggers early neutrophil infiltration in human pancreas allograft reperfusion. *Transplant Proc.* 2009; 41:3622–3627. [PubMed: 19917355]
- Wu JS, Cheung WM, Tsai YS, Chen YT, Fong WH, Tsai HD, Chen YC, Liou JY, Shyue SK, Chen JJ, Chen YE, Maeda N, Wu KK, Lin TN. Ligand-activated peroxisome proliferator-activated receptor-gamma protects against ischemic cerebral infarction and neuronal apoptosis by 14-3-3 epsilon upregulation. *Circulation.* 2009a; 119:1124–1134. [PubMed: 19221220]
- Wu R, Zhou M, Dong W, Ji Y, Miksa M, Marini CP, Ravikumar TS, Wang P. Ghrelin hyporesponsiveness contributes to age-related hyperinflammation in septic shock. *Ann Surg.* 2009b; 250:126–133. [PubMed: 19561473]
- Yu JH, Kim KH, Kim H. SOCS 3 and PPAR-gamma ligands inhibit the expression of IL-6 and TGF-beta1 by regulating JAK2/STAT3 signaling in pancreas. *Int J Biochem Cell Biol.* 2008; 40:677–688. [PubMed: 18035585]
- Zeng HK, Wang QS, Deng YY, Jiang WQ, Fang M, Chen CB, Jiang X. A comparative study on the efficacy of 10% hypertonic saline and equal volume of 20% mannitol in the treatment of experimentally induced cerebral edema in adult rats. *BMC Neurosci.* 2010; 11:153. [PubMed: 21143951]
- Zhang HL, Xu M, Wei C, Qin AP, Liu CF, Hong LZ, Zhao XY, Liu J, Qin ZH. Neuroprotective effects of pioglitazone in a rat model of permanent focal cerebral ischemia are associated with peroxisome proliferator-activated receptor gamma-mediated suppression of nuclear factor-kappaB signaling pathway. *Neuroscience.* 2011; 176:381–395. [PubMed: 21185913]
- Zimmerman SW, Manandhar G, Yi YJ, Gupta SK, Sutovsky M, Odhiambo JF, Powell MD, Miller DJ, Sutovsky P. Sperm proteasomes degrade sperm receptor on the egg zona pellucida during mammalian fertilization. *PLoS One.* 2011; 6:e17256. [PubMed: 21383844]

**HIGHLIGHTS**

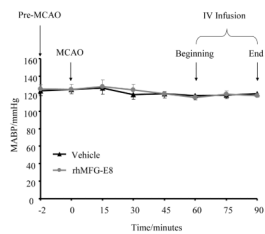
- Inflammation and apoptosis contribute to the pathogenesis of cerebral infarction
- rhMFG-E8 decreases infarct size and neurological deficits after cerebral ischemia
- rhMFG-E8 suppresses cytokine release and apoptosis after cerebral ischemia
- rhMFG-E8 is a novel neuroprotectant in cerebral ischemia



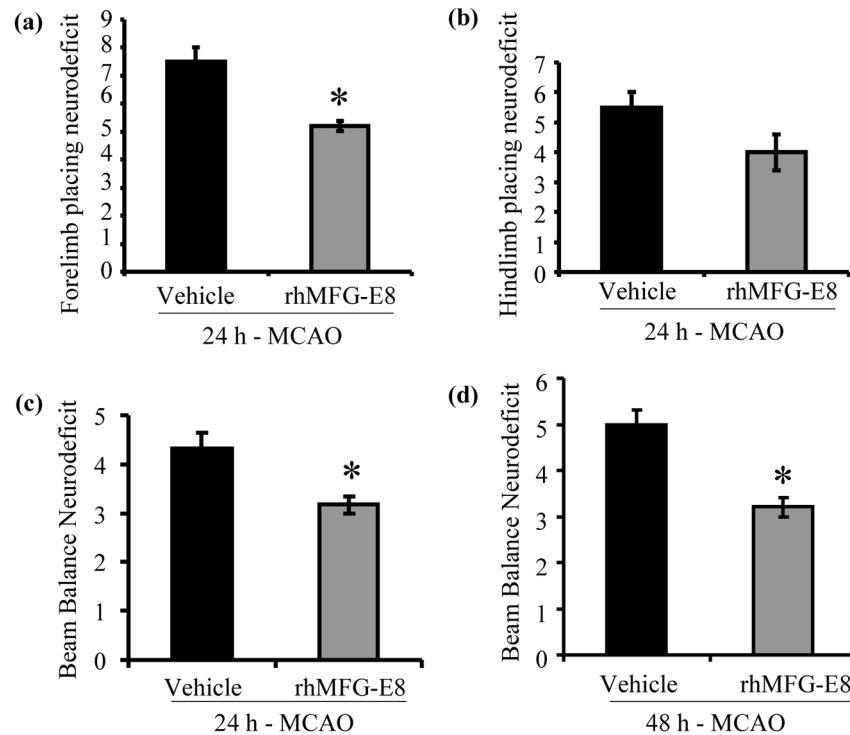
**Figure 1.**

Alteration in cerebral MFG-E8 protein level and gene expression after permanent focal cerebral ischemia by middle cerebral artery occlusion (MCAO). **(a)** Cerebral MFG-E8 protein levels were measured by Western blot at 24 h post-MCAO. Data are presented as mean $\pm$ SE, and analyzed by Student's t-test. Compared with Sham, cerebral ischemia (MCAO) decreased MFG-E8 levels (n = 4–5, \* $p < 0.05$  vs. **(b)**Sham). Cerebral MFG-E8 gene expression was measured at 24 h post-MCAO by real-time PCR. Data are presented as mean $\pm$ SE, and analyzed by Student's t-test. Cerebral ischemia did not cause a significant alteration in MFG-E8 gene expression (n = 4).

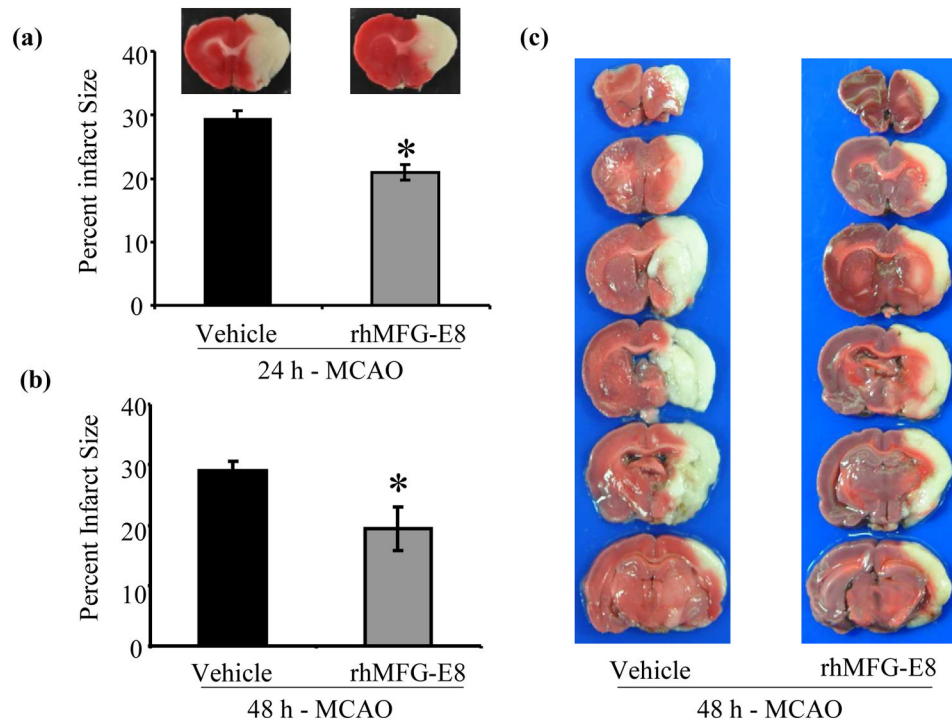




**Figure 2.** rhMFG-E8 does not alter blood pressure after cerebral ischemia. Mean arterial blood pressure (MABP) was monitored continuously by right femoral artery catheterization, starting from just before MCAO to 90 minutes post-MCAO. Data are presented as mean  $\pm$ SE, and analyzed by Student's t-test. In both vehicle and rhMFG-E8 treatment groups there was no significant change in MABP throughout the whole period of monitoring. Intravenous administration of rhMFG-E8, commencing at 60 minutes post-MCAO did not cause significant alteration of MABP compared with vehicle (n = 5)

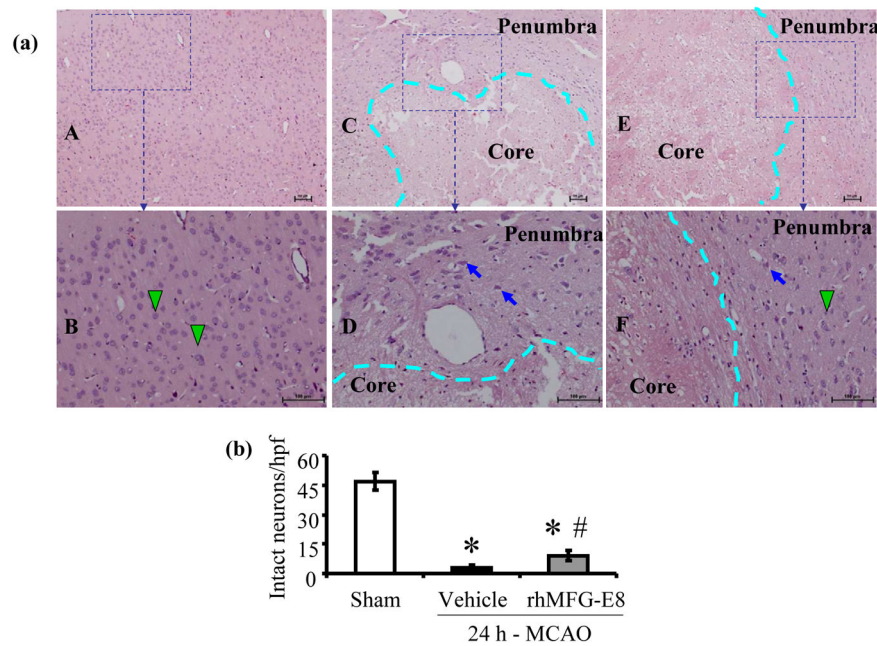


**Figure 3.** rhMFG-E8 treatment decreases sensorimotor and vestibulomotor deficits at 24 h and 48 h after permanent focal cerebral ischemia. **(a)** Left forelimb sensorimotor deficits were assessed by the forelimb placing test. Data are presented as mean±SE, and analyzed by Student's t-test. rhMFG-E8 treatment significantly reduced the sensorimotor deficit at 24 h post MCAO compared with vehicle (n = 5, \* $p < 0.05$  vs. Vehicle). **(b)** Left hindlimb sensorimotor deficit was measured by the hindlimb placing test. Data are presented as mean ±SE, and analyzed by Student's t-test. There was no statistical difference in hindlimb sensorimotor deficit between rhMFG-E8 treatment and vehicle at 24 h post-MCAO (n = 5). **(c)** Vestibulomotor deficit was assessed at 24 h after onset of cerebral ischemia by the beam balance test. Data are presented as mean±SE, and analyzed by Student's t-test. Compared with vehicle, rhMG-E8 treatment decreased the vestibulomotor deficit at 24 h post-MCAO (n = 5, \* $p < 0.05$  vs. Vehicle). **(d)** Vestibulomotor deficit was assessed at 48 h after onset of cerebral ischemia by the beam balance test. Data are presented as mean±SE, and analyzed by Student's t-test. The vestibulomotor deficit was significantly reduced at 48 h post-MCAO by rhMFG-E8 treatment compared with vehicle (n = 5, \* $p < 0.05$  vs. Vehicle).



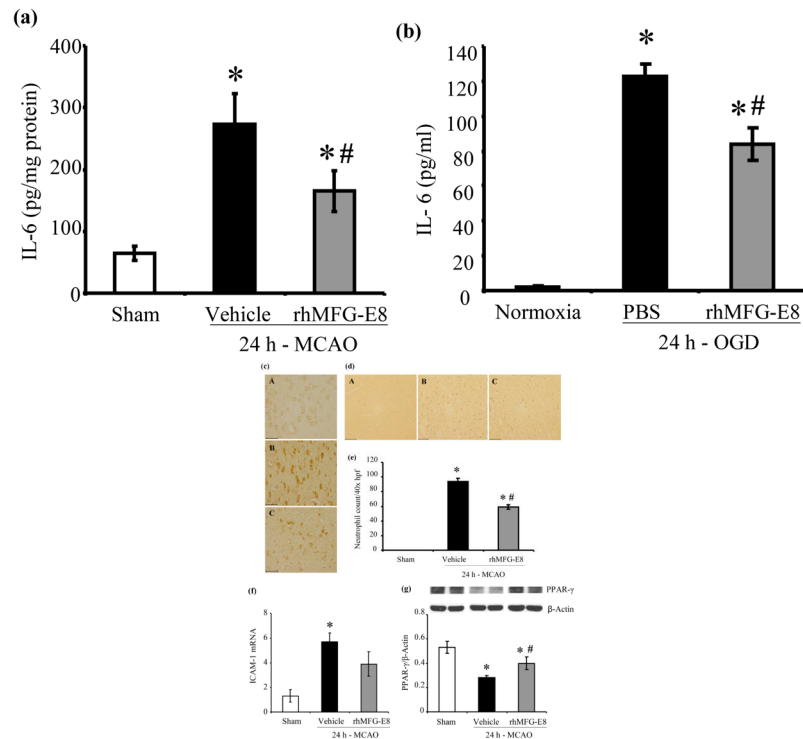
**Figure 4.**

The effect of rhMFG-E8 on infarct size after 24 h and 48 h permanent focal cerebral ischemia. 2 mm thick coronal slices of fresh brain tissue were stained with triphenyl tetrazolium chloride (TTC) and digitally analyzed with NIH ImageJ software. Data are presented as mean $\pm$ SE, and analyzed by Student's t-test. **(a)** Treatment with rhMFG-E8 decreased infarct size at 24 h post-MCAO compared with Vehicle ( $n = 6$ ,  $*p < 0.05$  vs. Vehicle). **(b)** rhMFG-E8 treatment decreased infarct size at 48 h post-MCAO compared with Vehicle ( $n = 6$ ,  $*p < 0.05$  vs. Vehicle). **(c)** Representative TTC staining of rostrally-caudally sectioned rat brains at 48 h post-MCAO shows that the vehicle grouped developed larger cerebral infarcts.



**Figure 5.**

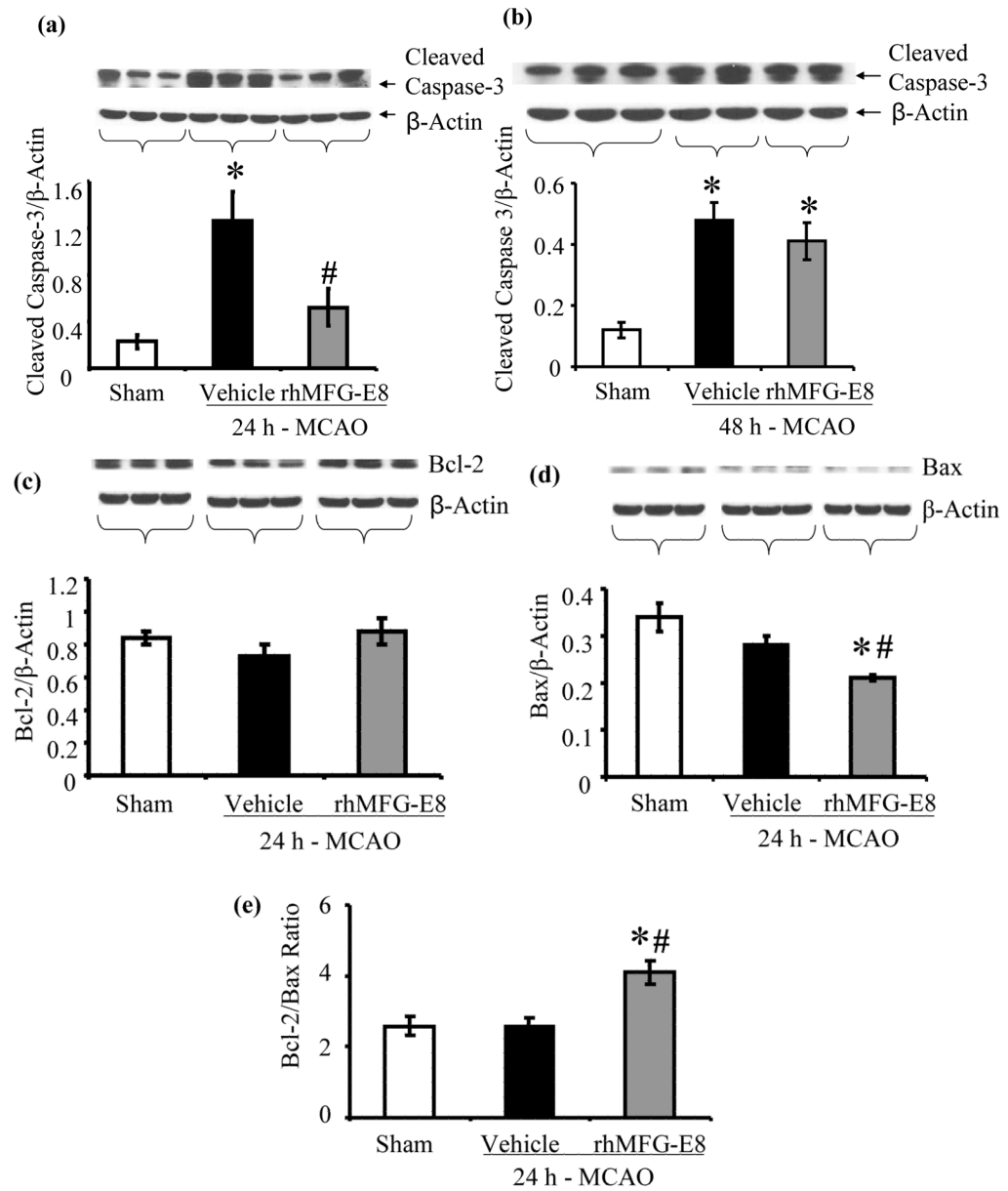
Histopathological changes after 24 h permanent cerebral ischemia. Hematoxylin-eosin (H&E) stained slides of rat brain sections were examined under bright field microscopy. (a) Slides were first examined at 40 $\times$  original magnification to delineate the ischemic core from the penumbra (delineation indicated by dashed cyan line) [Sham (A), Vehicle (C), and rhMFG-E8 (E)]. Scale bar = 100  $\mu$ m. An area was then selected in the penumbra and examined at a higher magnification of 100 $\times$  to show intact basophilic neurons (*green arrow heads*) and necrotic eosinophilic neurons (*blue short arrows*). Sham (B) shows intact basophilic neurons and rhMFG-E8 (F) shows more intact neurons in the penumbra compared with Vehicle (D). Scale bar = 100  $\mu$ m. (c) Intact neuron (basophilic neuron) counts were done at a higher magnification of 400 $\times$ . The average number of intact neurons in six images taken from six fields in the penumbra per slide, one slide per animal, was determined. Data are presented as mean $\pm$ SE, and analyzed by Kruskal-Wallis one-way ANOVA. Cerebral ischemia (MCAO) caused significant reduction in number of intact neurons in both Vehicle and rhMFG-E8 treated animals compared with Sham animals. rhMFG-E8 treatment protected neurons against necrosis compared with vehicle ( $n = 6$ ,  $*p < 0.05$  vs. Sham,  $\# p < 0.05$  vs. Vehicle).



**Figure 6.**

The effect of rhMFG-E8 on inflammatory cytokine secretion, neutrophil infiltration, and PPAR $\gamma$  levels in 24 h cerebral ischemia. **(a)** Cerebral IL-6 levels were measured by ELISA at 24 h post-MCAO. Data are presented as mean $\pm$ SE, and analyzed by one-way ANOVA and Student Newman Keul's method. Cerebral ischemia (MCAO) caused elevation of IL-6 levels in both Vehicle and rhMFG-E8 treated animals compared with Sham animals. Treatment with rhMFG-E8 downregulated IL-6 expression compared with Vehicle ( $n = 6$ ,  $*p < 0.05$  vs. Sham,  $\#p < 0.05$  vs. Vehicle). **(b)** IL-6 ELISA was performed on supernatants obtained from BV2 microglia 24 h oxygen-glucose deprivation (OGD), without re-oxygenation. Cells were plated in triplicates in three independent experiments. Data is presented as the mean (of the averages of the three experiments) $\pm$ SE, and analyzed by one-way ANOVA and Student Newman Keul's method. 24 h-OGD resulted in elevation of IL-6 levels, and rhMFG-E8 significantly decreased IL-6 secretion in all three experiments compared with vehicle ( $n = 3$ ,  $*p < 0.05$  vs. Sham,  $\#p < 0.05$  vs. Vehicle). **(c)** Brain tissue was immunohistochemically stained for TNF- $\alpha$  and examined at 400 $\times$  original magnification under bright field microscopy. Vehicle (B) and rhMFG-E8 (C) treated animals showed increased expression of TNF- $\alpha$  compared with Sham animals (A). rhMFG-E8 treatment (C) decreased TNF- $\alpha$  expression compared with Vehicle (B). Scale bar = 50  $\mu$ m. **(d)** Brain tissue immunohistochemically stained for the neutrophil marker, myeloperoxidase, and examined under bright field microscopy at 400 $\times$  original magnification. Sham (A) animals showed no staining for myeloperoxidase (no neutrophil infiltration) whereas Vehicle (B) and rhMFG-E8 (C) treated animals showed staining for myeloperoxidase. rhMFG-E8 treatment (C) after cerebral ischemia decreased myeloperoxidase staining compared with Vehicle (B). Scale bar = 50  $\mu$ m. **(e)** Quantification of cerebral neutrophil infiltration by myeloperoxidase immunohistochemistry. Neutrophils were identified as small, round, myeloperoxidase-staining cells on bright field microscopy at 400 $\times$  original magnification. The average number of neutrophils in six random fields per slide was determined as neutrophil count/40 $\times$  high power field (hpf). Data are presented as mean $\pm$ SE, and analyzed by one-way ANOVA and Student Newman Keul's method. Compared with Sham animals, Vehicle and rhMFG-

E8 treated animals showed increased neutrophil infiltration. rhMFG-E8 treatment decreased cerebral neutrophil infiltration compared with vehicle ( $n = 4$ ,  $*p < 0.05$  vs. Sham,  $\#p < 0.05$ , vs. Vehicle). **(f)** Cerebral ICAM-1 gene expression was measured by RT-PCR. Data are presented as mean $\pm$ SE, and analyzed by one-way ANOVA and Student Newman Keul's method. Cerebral ischemia resulted in upregulation of ICAM-1 expression in Vehicle compared with Sham. rhMFG-E8 treatment decreased ICAM-1 expression, even though not significant compared with Vehicle ( $n = 4-6$ ,  $*p < 0.05$  vs. Sham). **(b)** PPAR- $\gamma$  protein levels were determined by Western blot at 24 h post-MCAO. Data are presented as mean $\pm$ SE, and analyzed by Kruskal-Wallis one-way ANOVA. Compared with Sham, cerebral ischemia downregulated PPAR- $\gamma$  in the Vehicle group. rhMFG-E8 treatment upregulated PPAR- $\gamma$  expression compared with Vehicle ( $n = 6$ ,  $*p < 0.05$  vs. Sham,  $\#p < 0.05$  vs. Vehicle).



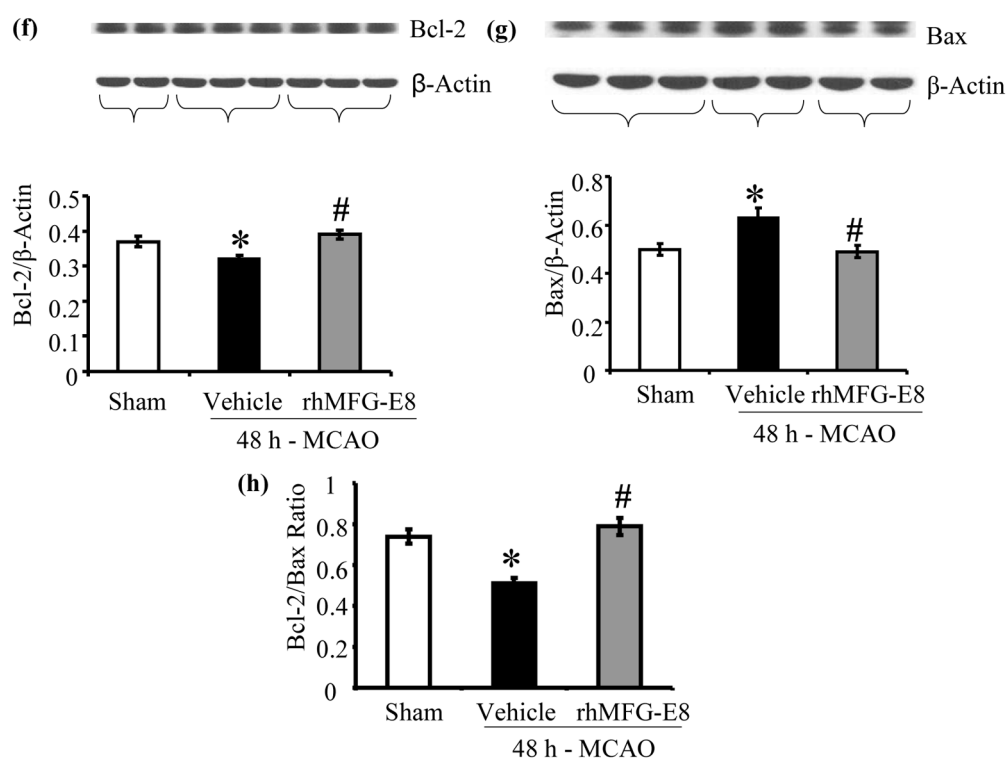


**Figure 7.** rhMFG-E8 treatment suppresses apoptosis in cerebral ischemia by downregulating cleaved caspase-3, bax, and upregulating bcl-2 and bcl-2/bax ratio. All data are presented as mean  $\pm$ SE, and analyzed by one-way ANOVA and Student-Newman Keul's method. (a) Cleaved caspase-3 was measured by Western blot at 24 h post-MCAO. 24 h - MCAO resulted in elevation of cleaved caspase-3 in the Vehicle. rhMFG-E8 decreased cleaved caspase-3 to levels similar to sham (n = 5–6, \* $p$  < 0.05 vs. Sham, # $p$  < 0.05 vs. Vehicle). (b) Cleaved caspase-3 levels at 48 h after cerebral ischemia; rhMFG-E8 showed a trend of decreasing cleaved caspase-3, even though not statistically different from vehicle (n = 5). (c) Bcl-2 levels in 24 h MCAO; There was no statistically significant difference in bcl-2 levels, even though rhMFG-E8 showed a trend of increasing bcl-2 (n = 6). (d) Bax levels in 24 h MCAO; Bax levels were similar between sham and vehicle at 24 h post-MCAO. rhMFG-E8 significantly downregulated bax compared with Sham and Vehicle (n = 6, \* $p$  < 0.05 vs. Sham, # $p$  < 0.05 vs. Vehicle). (e) Bcl-2/Bax ratio at 24 h post-MCAO; The Bcl-2/Bax ratio was not different between Vehicle and Sham at 24 h post-MCAO. rhMFG-E8 treatment significantly elevated Bcl-2/Bax ratio compared with Vehicle and Sham (n = 6, \* $p$  < 0.05 vs. Sham, # $p$  < 0.05). (f) Bcl-2 levels in 48 h MCAO; Bcl-2 was significantly reduced in the Vehicle group compared with Sham. rhMFG-E8 upregulated bcl-2 compared with vehicle (n = 5, \* $p$  < 0.05 vs. Sham, # $p$  < 0.05 vs. Vehicle). (g) Bax levels in 48 h MCAO; Bax was significantly upregulated in the Vehicle compared with Sham. rhMFG-E8 downregulated bax compared with Vehicle (n = 5, \* $p$  < 0.05 vs. Sham, # $p$  < 0.05 vs. Vehicle). (h) Bcl-2/Bax ratio at 48 h post-MCAO; Bcl-2/Bax ratio was downregulated compared with Sham. rhMFG-E8 treatment significantly upregulated the bcl-2/bax ratio (n = 5, \* $p$  < 0.05 vs. Sham, # $p$  < 0.05 vs. Vehicle).



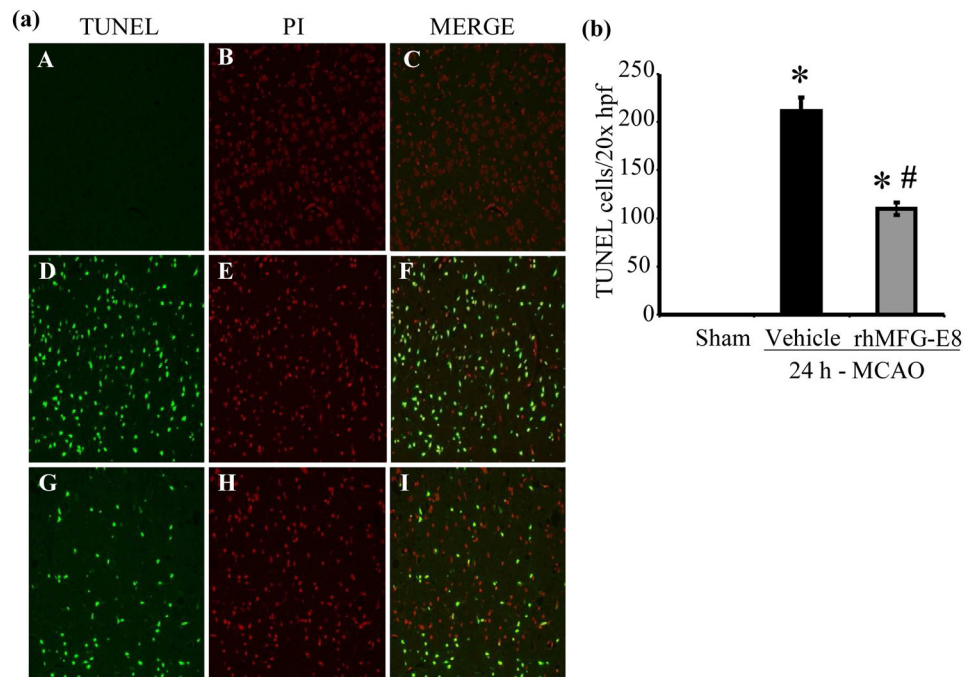


**Figure 8.**

(a) TUNEL staining after cerebral ischemia. On fluorescent microscopy at 200× original magnification, TUNEL positive cells appeared as green fluorescent while propidium iodide (PI) staining (red fluorescent) showed the nuclear location of the TUNEL reaction products. The Sham group (A, B, C) showed no TUNEL positive cells. Treatment with rhMFG-E8 (G, H, I) decreased TUNEL staining compared with Vehicle (D, E, F). (b) Quantification of TUNEL staining; Eight random fields were captured at 200× original magnification for each slide. The average number of TUNEL positive cells were counted and expressed as TUNEL cells/20× high power field (hpf). Data are presented as mean±SE, and analyzed by one-way ANOVA and Student Newman Keul's method. Treatment with rhMFG-E8 decreased the number of TUNEL positive cells compared with Vehicle group (n = 4, \* $p < 0.05$  vs. Sham, # $p < 0.05$  vs. Vehicle).

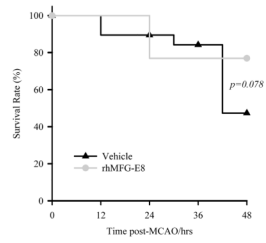


**Figure 9.** 48 h survival analysis. Survival rate was estimated by Kaplan-Meier LogRank analysis. The mortality in the Vehicle group started earlier compared with the rhMFG-E8 group. rhMFG-E8 resulted in a survival rate of 77% compared with 50% for Vehicle group (Vehicle, n = 20; rhMFG-E8, n = 13;  $p=0.078$ ).